Atmos. Chem. Phys. Discuss., 14, 22677–22713, 2014
www.atmos-chem-phys-discuss.net/14/22677/2014/
doi:10.5194/acpd-14-22677-2014

Atmospheric Chemistry and Physics Discussions
Open Access

The regime of aerosol asymmetry parameter over Europe, Mediterranean and Middle East based on MODIS satellite data: evaluation against surface AERONET measurements

M. B. Korras-Carraca[1], N. Hatzianastassiou[2], C. Matsoukas[1], A. Gkikas[2], and C. D. Papadimas[2]

[1]Department of Environment, University of the Aegean, 81100 Mytilene, Greece
[2]Laboratory of Meteorology, Department of Physics, University of Ioannina, 45110 Ioannina, Greece

Received: 10 May 2014 – Accepted: 27 July 2014 – Published: 5 September 2014

Correspondence to: N. Hatzianastassiou (nhatzian@cc.uoi.gr)

Published by Copernicus Publications on behalf of the European Geosciences Union.

Abstract

Atmospheric particulates are a significant forcing agent for the radiative energy budget of the Earth-atmosphere system. The particulates' interaction with radiation, which defines their climate effect, is strongly dependent on their optical properties. In the present work, we study one of the most important optical properties of aerosols, the asymmetry parameter (g_{aer}), in the region comprised of North Africa, the Arabian peninsula, Europe, and the Mediterranean basin. These areas are of great interest, because of the variety of aerosol types they host, both anthropogenic and natural. Using satellite data from the collection 051 of MODIS (MODerate resolution Imaging Spectroradiometer, Terra and Aqua), we investigate the spatio-temporal characteristics of the asymmetry parameter. We generally find significant spatial variability, with larger values over regions dominated by larger size particles, e.g. outside the Atlantic coasts of north-western Africa, where desert-dust outflow is taking place. The g_{aer} values tend to decrease with increasing wavelength, especially over areas dominated by small particulates. The intra-annual variability is found to be small in desert-dust areas, with maximum values during summer, while in all other areas larger values are reported during the cold season and smaller during the warm. Significant intra-annual and inter-annual variability is observed around the Black Sea. However, the inter-annual trends of g_{aer} are found to be generally small.

Although satellite data have the advantage of broad geographical coverage, they have to be validated against reliable surface measurements. Therefore, we compare satellite-based values with g_{aer} values measured at 69 stations of the global surface network AERONET (Aerosol Robotic Network), located within our region of interest. This way, we provide some insight on the quality and reliability of MODIS data. We report generally better agreement at the wavelength of 870 nm (correlation coefficient R up to 0.47) while of all wavelengths the results of the comparison were better for spring and summer.

1 Introduction

Atmospheric aerosol particles interact with radiation, mainly the short wave (SW or solar) part of the spectrum, modifying the energy budget of the Earth-atmosphere system. The aerosol effect is either direct, through the scattering and absorption of solar radiation, and thus reducing the incoming solar radiation flux at the surface, indirect, through the modification of cloud properties, or semi-direct, due to the absorption of solar radiation and consequent modification of the atmospheric temperature profile, convection, and cloud properties (e.g. Graßl, 1979; Hansen, 1997; Lohmann and Feichter, 2005).

The interaction of particles with the solar flux, which defines their climate role, strongly depends on their optical properties (Hatzianastassiou et al., 2004), whose availability cannot be ensured globally by surface in situ measurements. Besides the aerosol optical depth (AOD), which provides a good measure of the aerosol load over an area, one of the most important optical properties of atmospheric particles, which is used in radiative transfer, climate, and general circulation models, is the asymmetry parameter (g_{aer}). The asymmetry parameter describes the angular distribution of the scattered radiation and determines whether the particles scatter radiation preferentially to the front or back. The globally available satellite based AOD data are considered to a great extent reliable and adequate, due to significant developments in surface and satellite measurements during the last two decades, and particularly after 2000. On the other hand, despite the important role of the asymmetry parameter, relevant global coverage data are measured only for the last few years, or are available in long-term aerosol climatologies such as Global Aerosol Data Set (GADS, Koepke et al., 1997) and Max Planck Aerosol Climatology (MAC, Kinne et al., 2013). Even so, asymmetry parameter data are usually examined for regions with limited geographical extent and temporal coverage (Di Iorio et al., 2003), without intercomparison between alternative data platforms.

The goal of the present work is the study of the spatiotemporal distribution of the aerosol asymmetry parameter, using the most recent data from MODIS (MODerate

ACPD
14, 22677–22713, 2014

resolution Imaging Spectroradiometer, collection 051). Emphasis is given to the comparison between the provided MODIS data and respective reliable surface measurements of the global AERONET network, in order to gain insight on the quality of the former.

For this study we focus on the region defined by latitudes 5° N to 70° N and longitudes 25° W to 60° E, including North Africa, the Arabian peninsula, Europe, and the greater Mediterranean basin (Fig. 1). This area is selected because of the simultaneous presence of a variety of aerosol particles, both natural and anthropogenic (e.g. desert dust, marine, biomass burning, anthropogenic urban/industrial pollution) as shown in previous studies (Lelieveld et al., 2002; Sciare et al., 2003; Pace et al., 2006; Lyamani et al., 2006; Gerasopoulos et al., 2006; Kalivitis et al., 2007). This is due to the fact that two of the largest deserts of the planet are included in our area of interest, i.e. the Arabian desert and the Sahara, while one finds also significant sources of anthropogenic pollution, mainly in the European continent, with urban and industrial centres. Moreover, our area of interest and primarily its desert areas, are characterised by a large aerosol load (large optical depth, Remer et al., 2008). Finally, significant regions in this area, more specifically the Mediterranean basin and North Africa, are considered climatically sensitive, since they are threatened by desertification (IPCC, 2007, 2013). This is the first study (to our knowledge) that focuses on asymmetry parameter over a geographically extended area, while at the same time compares satellite with ground-station data.

2 Data

Daily data of the aerosol asymmetry parameter (g_{aer}) are used for the needs of this work. In order to achieve the largest geographical coverage of the studied region, we employ satellite data from the MODIS-Terra and MODIS-Aqua datasets. These data are compared with in-situ measurements at stations of the AERONET. We provide a detailed description of the utilised data in the following sections.

ACPD
14, 22677–22713, 2014

2.1 Satellite MODIS Terra and Aqua data

MODIS is an instrument (radiometer) placed on the polar-orbiting satellites of NASA (National Aeronautics and Space Administration) Terra and Aqua, 705 km from the Earth, in the framework of the Earth Observing System (EOS) programme. Terra was launched on 18 December 1999, while Aqua was launched on 4 May 2002. The two satellites are moving on opposite directions and their local equatorial crossing times are at 10.30 a.m. (Terra) and 13.30 p.m. (Aqua). MODIS is recording data in 36 spectral channels between the visible and the thermal infrared (0.44–15 µm), while its swath width is of the order of 2330 km, which results in almost full planetary coverage on a daily basis. The global MODIS database is generally considered as one of the most reliable at present.

Aerosol properties are monitored in 7 spectral channels between 0.47 and 2.13 µm and final results are derived through algorithms developed for aerosol quantities both over land and ocean (Kaufman et al., 1997; Tanré et al., 1997; Ichoku et al., 2002; Remer et al., 2005). MODIS data are organised in "collections" and "levels". Collections comprise data produced by similar versions of the inversion algorithms, with the most recent publically being "051" for both Terra and Aqua, which includes also outputs from the "Deep Blue" algorithm. Levels are characterised by data of different spatial and temporal resolution.

In this study we use daily MODIS data for the asymmetry parameter g_{aer} provided on an $1^{\circ} \times 1^{\circ}$ grid (namely about 100 × 100 km), from the most recent Collection 051, Level 3. These data were measured at wavelengths 470, 660, and 870 nm (for which corresponding AERONET gaer data also exist), only over oceanic regions, since they were derived through the algorithm for aerosol properties over the ocean. The period of analysis stretches from 24 February 2000 to 22 September 2010 for MODIS-Terra and from 4 July 2002 to 18 September 2010 for MODIS-Aqua.

2.2 Ground based AERONET data

AERONET (AErosol RObotic NETwork) is a global network of stations focused on the study of aerosol properties. AERONET currently encompasses about 970 surface stations (number continuously evolving) equipped with sun photometers of type CIMEL Electronique 318 A (Holben et al., 1998), which take spectral radiation flux measurements.

The optical properties of aerosols are extracted through the application of inversion algorithms (Dubovik and King, 2000). Data are provided on three levels (1.0, 1.5, and 2). In the present work, we use the most reliable Level 2 data, due to their being cloud-screened and quality-assured. AERONET derives the asymmetry parameter at wavelengths 440, 675, 870, and 1020 nm. We employ daily Level 2 asymmetry parameter data from 69 stations (Fig. 1) contained in our study area (N. Africa, Arabian peninsula, Europe). We choose only coastal stations, in order to ensure the coexistence of satellite marine g_{aer} data with surface data. Also, in order to compare corresponding data between the satellite and station platforms, we perform comparison only for the 440, 675 and 870 nm wavelengths.

3 Satellite based results

3.1 Geographical distributions

The spatial distribution of annual mean values of g_{aer} is given in Fig. 2 separately at the wavelengths 470, 660 and 870 nm. The values are averages over the common period between Terra and Aqua, namely 4 July 2002 till 18 September 2010. A significant spatial variability is evident, with MODIS-Terra values varying within the ranges 0.63–0.76, 0.57–0.75, and 0.55–0.74, at 470, 660 and 870 nm, respectively. The results exhibit a decreasing tendency of g_{aer} with increasing wavelength, consistent with the theory. Similar results are also obtained from MODIS-Aqua, but with slightly smaller values

ACPD
14, 22677–22713, 2014

Evaluation of MODIS aerosol asymmetry against AERONET measurements

M. B. Korras-Carraca et al.

than Terra by up to 0.02 on average. More specifically, the corresponding ranges of wavelengths are 0.63–0.75, 0.57–0.73, and 0.55–0.73. The smaller Aqua than Terra g_{aer} values could be attributed to smaller sizes of aerosols in midday than morning, corresponding to passages of Aqua and Terra, respectively, associated with lower relative humidity values and shrinking of aerosol particles. Such diurnal variation has been also reported for AOD (Smirnov et al., 2002; Pandithurai et al., 2007), but either decreasing or increasing in the day because of the influence of other factors too, e.g. emissions or wind conditions, apart from aerosol hygroscopicity.

In general, the largest g_{aer} values (deep red colors) are observed off the coasts of West Africa (eastern tropical Atlantic Ocean) at all three wavelengths. High values are also found over the Red and Arabian Seas. These high values are due to strong dust outflows from the Saharan and Arabian deserts carrying out coarse aerosol particles causing strong forward scattering. Nevertheless, the Persian Gulf region, which is surrounded by deserts, is characterized by relatively smaller g_{aer} values. More specifically, values as small as 0.69 (MODIS-Terra) and 0.67 (MODIS-Aqua) are observed in this region at 470 nm, while at the longer wavelengths (660, 870 nm) the smallest values are equal to 0.66 (Terra) and 0.64 (Aqua). The smaller g_{aer} values over the Persian Gulf can be attributed to the presence of fine aerosols, which is corroborated by the low effective radius and large fine-fraction measurements by MODIS over the Persian Gulf, compared to neighbouring areas (not shown here). These fine particles originate from the industrial activities in the Gulf countries related to oilfields or refineries (Goloub and Arino, 2000; Smirnov et al., 2002a, b; Dubovik et al., 2002).

The high g_{aer} values over the northeastern tropical Atlantic Ocean as well as west of the Iberian coasts are possibly related with the presence of coarse sea salt and transported dust particles. On the other hand, the asymmetry parameter takes clearly smaller values over the Black Sea, where according to MODIS-Terra varies between 0.63 and 0.7 at 470 nm, 0.57 and 0.67 at 660 nm, and 0.55 and 0.66 at 870 nm (corresponding maximum Aqua values are smaller by 0.02), with the smallest values appearing in the Crimean peninsula. The small Black Sea g_{aer} values can be associated with

ACPD
14, 22677–22713, 2014

Title Page
Abstract | Introduction
Conclusions | References
Tables | Figures
◀| |▶
◀ ▶
Back | Close
Full Screen / Esc
Printer-friendly Version
Interactive Discussion

the vicinity of industrial but also biomass burning activities in nearby countries. A region of special interest is the Mediterranean basin since it hosts a large variety of aerosols like anthropogenic, desert dust or sea salt (e.g. Barnaba and Gobbi, 2004). The MODIS results over this region show relatively small g_{aer} values, secondary to those of Black Sea, characterized by an increase from north to south, which is more evident at 660 and 870 nm. More specifically, based on MODIS-Terra, g_{aer} over the Mediterranean takes values from 0.68 to 0.74 at 470 nm, while at 670 and 870 nm it ranges from 0.64 to 0.73 and 0.62 to 0.72, respectively. According to MODIS-Aqua the Mediterranean g_{aer} values are slightly smaller again. The observed low values in the northern parts of the Mediterranean are probably associated with the presence of fine anthropogenic aerosols transported from adjacent urban and industrial areas in the north, especially in central Europe. In contrast, the higher g_{aer} values in the southern Mediterranean, particularly near the North African coasts, can be explained by the proximity to the Sahara desert and the frequent transport of significant amounts of coarse dust (e.g. Kalivitis et al., 2006; Hatzianastassiou et al., 2009; Gkikas et al., 2009, 2013).

The spatial distributions of climatological monthly mean g_{aer} values from MODIS-Aqua at 470 nm reveal significant differences either as to the range or to the patterns of the seasonal variability, depending on the area (Fig. 3). Thus, in tropical and subtropical areas of Atlantic Ocean (up to about 30° N), where dust is exported from Sahara, g_{aer} keeps high values throughout the year, which reach or even exceed 0.74 locally. Over the regions of Arabian and Red Seas and the Gulf of Aden, which also experience desert dust transport, larger g_{aer} values appear in the period from March to September, with a maximum on August (locally as high as 0.75–0.76). This seasonal behavior is in line with intra-annual changes of dust production over the Arabian peninsula, as indicated primarily by MODIS Angström Exponent (AE) and secondarily by Deep Blue aerosol optical depth data and also as reported in the literature (Prospero et al., 2002). Indeed, the production of dust there is relatively poor in winter, increases in March and April and becomes maximum in June and July (Prospero et al., 2002). Over the Arabian Sea, it is known that large amounts of desert dust are carried out

ACPD
14, 22677–22713, 2014

Evaluation of MODIS aerosol asymmetry against AERONET measurements

M. B. Korras-Carraca et al.

during spring and early summer (Prospero et al, 2002; Savoie et al., 1987; Tindale and Pease, 1999; Satheesh et al., 1999). Nevertheless, according to MODIS, the seasonal variability of g_{aer} remains relatively small there in line with a small seasonal variability in MODIS Deep Blue AE data. This can be explained by the presence of sea salt coarse particles throughout the year, with which dust particles co-exist.

A greater seasonal variability exists over the Persian Gulf, where g_{aer} values are higher during spring and in particular in summer (up to 0.74 at 470 nm according to Aqua), and smaller in autumn and winter (area-minimum values smaller than 0.65). This seasonal behavior can be explained taking into account the meteorological conditions over the greater area of the Gulf; from June to September dry northwestern winds (Shamal) blow, carrying desert dust from the arid areas of Iraq (Heishman, 1999; Smirnov et al., 2002a, b). The transport of dust is gradually decreased in autumn, is minimum in winter and increases again in spring. When the presence of desert dust is limited, a significant fraction of total aerosol load in the region is consisted of fine anthropogenic particles (Smirnov et al., 2002a, b), which can explain the observed relatively small g_{aer} values in autumn and winter.

In the Mediterranean basin, g_{aer} exhibits a relatively small seasonal variation, though higher values tend to appear in summer and secondarily in early and late spring, in line with the stronger presence of transported dust in the area, transported from the Sahara desert (Gkikas et al., 2013). On the contrary, over the Black Sea, a clear seasonal cycle is apparent, with higher values in the cold period of the year and smaller in the warm one. More specifically, according to MODIS-Aqua, the values at 470 nm drop down to 0.61 in summer months whereas they reach 0.7 in January and December.

It is also interesting to look at the geographical distribution of monthly g_{aer} values in latitudes higher than 50° N, for which annual mean values were not given in Fig. 2 because of unavailability of data for all months. Off the coasts of northern France (English Channel) and Germany the asymmetry parameter has small values, with a non-significant annual course (note that values do not exist for January and February). In these areas, the aerosol load consists mainly of anthropogenic polluted particles, which explains the small g_{aer} values there.

In the Baltic Sea (values available from March to October) g_{aer} shows a significant spatial and temporal variability. More specifically, it is small during summer whereas it increases, locally up to more than 0.7, in March and October. The smaller summer values can be explained by the presence of fine aerosols in the Baltic Sea originating from forest fires in Europe and Russia (Zdun et al., 2011). On the contrary, in autumn the local aerosol loading consists largely of coarse marine aerosols. It is important to note that the Baltic Sea hosts significant amounts of anthropogenic industrial and urban aerosols throughout the year, but especially in summer (Zdun et al., 2011).

In the higher latitudes of Atlantic Ocean, where the presence of maritime aerosols is dominant, it is observed a remarkable month by month variation of asymmetry parameter, with low values in summer (values down to 0.59) against high values (up to 0.75–0.77) in spring (March, April) and autumn (October). This difference is possibly explained by the seasonal variability of aerosol size in the northern Atlantic. Apart from the presence of coarse sea salt throughout the year, in spring and summer small particles are formed through photochemical reactions of dimethylsulphide (DMS) emitted by phytoplankton decreasing the aerosol size. Moreover during summer fine anthropogenic aerosols are transported in the region from North America (Yu, 2003; Chubarova, 2009). These result in lower g_{aer} values between May and August.

Based on MODIS-Terra, the patterns of spatial distribution are generally the same with Aqua, but with slightly larger g_{aer} values. At larger wavelengths (660, 870 nm) it is observed a decrease of g_{aer}, in particular of its smallest values. Further details and also an overall picture will be given later on, in the Sect. 3.2.1 which deals with climatological monthly mean values not at the pixel but regional level.

ACPD
14, 22677–22713, 2014

3.2 Temporal variability

3.2.1 Seasonal variability

In order to provide an easier assessment of the seasonal cycle of aerosol asymmetry parameter and its changes from a region to another, but also among the different wavelengths (470, 660 and 870 nm), the study region was divided in 6 smaller sub-regions (see Fig. 1). For each sub-region, the average values of monthly mean climatological data of the pixels found within each sub-region's geographical limits have been computed and are given in Fig. 4, for every wavelength and for Terra and Aqua. It appears that the seasonal cycle differs between the sub-regions, as it has been already shown in the geographical map distributions discussed in the previous section.

At 470 nm (Fig. 4i), the intra-annual variability of g_{aer} is greater over the Black Sea, where it is as large as 0.06 according to MODIS-Terra and 0.05 according to MODIS-Aqua, the north-eastern Atlantic Ocean (0.04 and 0.05 for Terra and Aqua, respectively) and the seas of North Europe (0.05 for both Terra and Aqua). In these regions, there is a tendency for smaller values during summer. More specifically, in the Black Sea the smallest g_{aer} value (0.64) is observed in June, over the seas of North Europe in July and over the north-eastern Atlantic Ocean in August. In these regions, the largest values appear in the cold period of the year. Reverse seasonality with a large seasonal amplitude is observed over the Persian Gulf, where the variability is as large as 0.08, according to both MODIS-Terra and Aqua. The seasonal cycle of g_{aer} over the Middle East exhibits a smaller range of variability (0.02 for MODIS-Terra and 0.03 for Aqua), with maximum values in summer and minimum in winter. In the other two sub-regions (Mediterranean and eastern tropical Atlantic Ocean) the annual range of values is small (<0.02). It is noteworthy that in the Mediterranean Sea, there is a weak tendency of appearance of double maxima in winter and spring. The spring maximum should be associated with the presence of desert dust particles, which are transported from Sahara, mainly in the eastern Mediterranean in this season (e.g. Fotiadi et al., 2006; Kalivitis et al., 2007; Papadimas et al., 2008; Gkikas et al., 2009; Hatzianastassiou

ACPD
14, 22677–22713, 2014

et al., 2009; Gkikas et al., 2013). There is also a similar transport of Saharan dust in the central and western Mediterranean during summer and autumn (e.g. Gkikas et al., 2009, 2013), but then the predominance is not so clear because of the co-existence of fine anthropogenic aerosols. Regardless of the annual cycle, smaller g_{aer} values are clearly distinguished over the Black Sea and North Europe seas throughout the whole year.

At 660 nm, the g_{aer} values are lower than at 470 nm, in particular over Black Sea, North Europe and North-East Atlantic, whereas the intra-annual variability (range of g_{aer} values) increases up to 0.1 (Terra) and 0.08 (Aqua) over the Black Sea. This increase is mainly attributed to the reduction of summer values due to the strong appearance of fine aerosols in this season. Also, at 660 nm, there is a clearer double annual variation of g_{aer} over the Mediterranean Sea than at 470 nm. At 870 nm the general picture is similar to that of 660 nm though a further increase of month by month variability is noticeable.

In general, our results indicate that over the regions characterized by a strong presence of desert dust particles (eastern Atlantic Ocean, and the Middle East and Mediterranean Seas) the annual range of variability of g_{aer} is smaller than in the other regions. An additional feature above regions with desert dust is the smaller decrease of g_{aer} values with increasing wavelengths, which can be attributed to the different spectral behavior of solar radiation scattering by fine and coarse aerosols (e.g. Dubovik et al., 2002; Bi et al., 2011).

It should be noted here that according to our results, using MODIS-Terra and Aqua data, the g_{aer} seasonal cycle is about similar but with generally greater larger Terra than Aqua values.

3.2.2 Inter-annual variability and changes

Figure 5 displays the geographical distribution of the slope of inter-annual trend of g_{aer} over the study region, as computed from the application of the Mann-Kendall test to time series of deseasonalized monthly anomalies of g_{aer} at 470 nm. Results are shown

ACPD
14, 22677–22713, 2014

in units decade^{-1} for both Terra and Aqua over their common time period, namely 2002–2010, only if the trend is statistically significant at the 95 % confidence level. We also performed the same analysis for the 660 and 870 nm (not shown), with similar results to the 470 nm wavelength.

In general, the estimated changes are relatively small. Terra produces widely statistically significant positive trends, showing that during the period of interest, the asymmetry parameter increased over the examined area, with very few exceptions. The results from Aqua are statistically significant at considerably fewer cells, but also give a few points with decreasing g_{aer}. Based on Terra data, the stronger increases are observed in the eastern and southern Black Sea, as well as over the Baltic and Barents Seas. According to MODIS-Aqua, negative changes are found over few Atlantic Ocean cells. Both Aqua and Terra report increases of g_{aer} over the Persian Gulf, the Red Sea, South Black Sea, East Mediterranean, the coast of the Iberian Peninsula, and some coastal areas of West Africa. The differences encountered between the Terra and Aqua g_{aer} trends may be attributed to the different time of passage of each satellite platform carrying the same MODIS instrument, given that everything else is the same. Therefore, other than aerosol paremeters which affect g_{aer}, like atmospheric relative humidity related to aerosol hygroscopicity, could be able to account for the differences between the Terra and Aqua trends. A relevant analysis would be helpful to this aim but it is beyond the scope of the present study.

The overall g_{aer} changes of Fig. 5 may hide smaller timescale variations of g_{aer}, which are obtained by the time-series shown in Fig. 6. Results are given for the 7 sub-regions defined previously, at the three different wavelengths and for Terra and Aqua separately. A general pattern is the decrease of g_{aer} values with increasing wavelength, in particular from 470 to 660 nm. The largest month to month and year to year variation is for Black Sea (Fig. 6i). Relatively large variability is also found in the sub-regions of NE Atlantic (6v), North Europe (6vi) and the Persian Gulf (6vii). On the contrary, small variability is noticed in the eastern Atlantic, where systematic dust outflows from Sahara take place leading to consistently high values of g_{aer}. There are also some other interesting patterns, like the significant drop of g_{aer} with wavelength in areas characterized by the presence of fine aerosols, namely the Black Sea, North Europe and the Persian Gulf (Fig. 6i, vi, vii, respectively). The specific patterns of inter-annual changes of g_{aer} are suggested by both Terra and Aqua, though a slight overestimation by Terra is again apparent in this figure. The obtained results of our analysis are meaningful and in accordance with the theory, underlining the ability of satellite observations to reasonably capture the g_{aer} regime over the studied regions.

4 Evaluation against AERONET data

In this section, we compare the satellite-based aerosol asymmetry parameter with measurements from the global network of surface stations of AERONET, which is considered as the reference dataset (Holben et al., 1998). For this purpose, we identified the AERONET stations inside our area of interest and finally utilised only the coastal ones, so that both satellite and surface data be available. The total number of these stations is 69, and their locations are shown in Fig. 1.

Table 1 contains the comparison statistical metrics for all wavelengths (Pearson correlation coefficient, bias, root mean squared error, slope, intercept) of the comparison between surface data from AERONET and satellite data from MODIS-Terra and MODIS-Aqua, which correspond to the $1^\circ \times 1^\circ$ cell wherein each station is located. For this analysis, we use all cells and days with common data between Terra-AERONET and Aqua-AERONET. The mean differences are calculated as g_{aer}(AERONET) – g_{aer}(Aqua) and g_{aer}(AERONET) – g_{aer}(Terra).

In general, we may note that on an annual level, the MODIS-Terra and Aqua asymmetry parameter values at 470 nm are not in very good agreement with the respective data from AERONET at 440 nm (correlation coefficients equal to 0.25 and smaller than 0.27, for Terra and Aqua respectively), while the results at the largest wavelengths are more reassuring, without being very satisfactory ($R \leq 0.42$ and 0.47 at 660/675 nm and 870 nm, respectively). At 870 nm (Table 1 and Fig. 7), correlation coefficients are found

ACPD
14, 22677–22713, 2014

to be the largest and equal to 0.47 (AERONET-Terra) and 0.46 (AERONET-Aqua), while satellite data are slightly overestimated compared to the surface data (bias −0.035 or 5.54 % and −0.015 or −2.43 %, respectively).

It is important to note that the agreement of satellite and surface data is better in spring and summer, for all studied wavelengths. Specifically, the correlation coefficients increase up to 0.35, 0.50 and 0.54 at 440/470 nm, 660/675 nm and 870 nm, respectively, while the bias decreases down to 0.0005 (0.07 %), 0.003 (0.46 %) and 0.007 (1.11 %), respectively.

Moreover, we find that for all seasons g_{aer} values at 870 nm and 660 nm, both from MODIS-Terra and MODIS-Aqua, are overestimated compared to $g_{aer(AERONET)}$ at the corresponding wavelengths (stronger overestimation at 870 nm and by Terra). Finally we note an underestimation of g_{aer} at 470 nm from MODIS-Aqua, relative to the data by AERONET at 440 nm, while very small biases (<0.5 %) are found between Terra and AERONET at the same wavelengths.

The applied least squares fit line to the scatterplot comparison between matched MODIS-AERONET data pairs (Fig. 7) indicates that MODIS overestimates g_{aer} at all but more in the smaller than larger values, i.e. more for fine than coarse particles.

We present the frequency distributions of asymmetry parameter daily values (Fig. 8) on the days when data from all three databases (MODIS-Terra, MODIS-Aqua and AERONET) were provided. Figure 8a corresponds to the whole area of interest, while Fig. 8b and c correspond to two broad sub-regions with basic differences in the aerosol source, namely Europe with great anthropogenic sources, and Africa, Middle East and Arabian peninsula, with predominant natural sources and mainly desert dust. There is an apparent skew in the MODIS-Terra and MODIS-Aqua g_{aer} distributions, while the AERONET distributions are more symmetrical. Moreover, the satellite data distributions show larger values and smaller standard deviations compared to AERONET, with the Terra overestimation being more exaggerated. The disagreement is more pronounced in the sub-region of Europe, while in the sub-region of North Africa/Arabian peninsula, the distributions of satellite and surface data agree more thus confirming the finding

ACPD
14, 22677–22713, 2014

of Fig. 7 (greater MODIS overestimation for fine than coarse particles) based on the slope of applied linear regression fit. Values over Europe are generally smaller than over North Africa/Arabian peninsula (Fig. 3), which can be attributed to the presence of larger size particles of desert origin in the latter sub-region, in contrast to Europe, where due to industrial activity and frequent biomass burning the presence of smaller size particles is important. Therefore, the smaller g_{aer} values (<0.6) in the frequency distributions of the whole area, are overwhelmingly contributed by the European sub-region, contrasting with larger values (0.7–0.75) being contributed by both sub-regions and even more by N. Africa/Arabian peninsula at larger g_{aer}.

Potentially useful results may be derived by the comparison of the temporal trends from satellite and surface data. We show in Fig. 9 the absolute and relative changes of the asymmetry factor, calculated through regression on monthly time series of g_{aer} at 9 AERONET stations (blue squares, Fig. 1) with satisfactory temporal coverage of data, selected to have recorded at least 40 monthly values. In the same figure, these temporal variations are compared with corresponding data from MODIS-Terra and MODIS-Aqua, from the 1×1 degree cells containing the locations of the 9 selected stations. We note that we only perform this analysis in a month only if all three datasets give data for the specific month. It should be noted that the g_{aer} changes for these stations do not refer to the same period but they all ensure a complete enough time period enabling thus the derivation of safe conclusions on how MODIS and AERONET changes compare to each other. At five out of the nine stations ("Barcelona", "Dhadnah", "Lecce University", "Rome Tor Vergata" and "Villefranche") the temporal tendencies have the same sign for all three databases, with AERONET showing larger trends. Moreover, the trends are statistically significant at the 95 % confidence level for "Barcelona" station.

The overall comparison between satellite and surface g_{aer} data performed in the scatterplot of Fig. 7 and Table 1 does not allow one to have an insight to how the comparison behaves spatially, namely how it differs from a region to another. This is addressed in Fig. 10, showing the comparison of satellite and surface data at the wavelength of 870 nm separately between MODIS-Terra – AERONET and MODIS-Aqua –

ACPD
14, 22677–22713, 2014

AERONET (Fig. 10b). For this comparison, we selected AERONET stations for which there is satisfactory overlap between the time series from AERONET and the time series from MODIS, namely the number of common days between AERONET-Terra and AERONET-Aqua is larger than 100. This intentionally selected less strict criterion that the one used in Fig. 9 is satisfied by 36 stations for AERONET-Terra and by 34 for AERONET-Aqua. For each AERONET station we compute and plot the Pearson correlation coefficient between the station data and the corresponding MODIS-Terra or Aqua data at 870 nm, for the $1^{\circ} \times 1^{\circ}$ cell containing the station. Moreover, there is the information if the trends between AERONET and either MODIS-Terra or Aqua have the same (blue color) or opposite (red color) sign.

In the case of the $g_{\mathrm{aer\,(AERONET)}} - g_{\mathrm{aer\,(Terra)}}$ comparison, at 5 stations the correlation coefficient R is larger than 0.5, while at 21 stations $0.3 < R < 0.5$. The largest R found is 0.64 at station "Bahrain". With respect to the agreement on the sign of the trends, at 24 out of 36 stations (67 %) there is a trend sign match and at 12 stations (33 %) a mismatch. A similar picture emerges for the comparison $g_{\mathrm{aer\,(AERONET)}} - g_{\mathrm{aer\,(Aqua)}}$. In this case, there are again 5 stations with $R > 0.5$ (maximum value $R = 0.61$ again at "Bahrain"), while at 19 stations $0.30 < R < 0.50$. Also, we see that at 22 stations there is a trend sign match and at 12 there is a mismatch (respective percentages equal to 65 % and 35 %).

5 Summary and conclusions

Using satellite data from the latest available collection (051) of MODIS-Terra and Aqua data, we examine the spatiotemporal variations of the aerosol asymmetry parameter over maritime areas adjacent to North Africa, the Arabian peninsula and Europe. Generally, the largest values of the asymmetry parameter, indicating the strongest forward scattering of radiation by atmospheric aerosols, are found over areas with aerosol load being dominated by large size particles of desert dust (tropical Atlantic, Arabian and Red Seas). On the contrary, smaller g_{aer} values are seen where a significant fraction

ACPD
14, 22677–22713, 2014

of aerosol load comes from small size particles of anthropogenic origin, e.g. over the Black Sea. The results are consistent with the theory and thus prove a good performance of the MODIS retrieval of aerosol asymmetry parameter. Depending on the area of interest, the seasonal cycle of the asymmetry parameter varies markedly. More specifically, in areas with abundance of desert dust particles, the range of intra-annual variation is small, with the largest values during summer, while in other areas the seasonality is reversed, with the largest values during the cold season and the smallest during the warm season. The asymmetry parameter decreases with wavelength, especially when one examines its spatially minimum values, while this decrease is weaker for the larger g_{aer} values, corresponding to the presence of coarser particles.

The seasonal fluctuation is more pronounced with increasing wavelength in the examined regions, which is attributed to the different spectral behaviour of the asymmetry parameter for small and large particles. With respect to the inter-annual variability of the asymmetry parameter, we did not discern very important either increasing or decreasing tendencies, with absolute changes smaller than 0.04 in any case. On the other hand, we found opposing tendencies for the two satellite datasets. MODIS-Terra observes mostly increasing tendencies, while Aqua gives regions with decreasing tendencies. Generally, the largest intra-annual and inter-annual variations are seen over the Black Sea, while the smallest over the tropical Atlantic.

We compare satellite data with surface data from the AERONET, in order to validate the reliability of the former. The quantitative comparison is very useful, since satellite data provide broad geographical coverage and are very important in any study related to aerosols and their climate impact. The disagreement with surface stations can give insights in the resulting errors. Through the examination of frequency distributions of daily g_{aer}, a shift of satellite data towards larger values relative to surface data becomes apparent. This finding is more pronounced for g_{aer} over Europe, while the North African, Arabian peninsula values are more in agreement. Moreover, the smallest g_{aer} values originate from particles from Europe, because of the generation of smaller size particles by industrial activities and biomass burning.

ACPD
14, 22677–22713, 2014

In this work we present scatter plots of daily g_{aer} values between MODIS-Terra, MODIS-Aqua, and AERONET, which show moderate agreement between satellite data at 470 nm and surface data at 440 nm, with small correlation coefficients ($R < 0.3$). Slightly better agreement was noted at larger wavelengths, but still without reaching very satisfactory levels ($R < 0.47$). Nevertheless, during spring and summer, satellite and surface measurements tend to agree more. Finally, for the comparisons at 660/675 and 870 nm, we report an overestimation of g_{aer} by MODIS compared to AERONET, as expected because of the less steep decrease of g_{aer} with wavelength of MODIS.

We extract pairs of daily Terra-AERONET and Aqua-AERONET values at stations with at least 100 common days. At 21 of 36 stations for Terra-AERONET comparison and at 19 of 34 stations for Aqua-AERONET comparison we derive $0.3 < R < 0.5$, while at 5 stations in both cases, the correlation coefficients are larger than 0.5. Finally, as far as the signs of temporal trends are concerned, we determine agreement in 67 % for the Terra-AERONET comparison and in 65 % of stations for Aqua-AERONET comparison.

The results of the present analysis are useful since they assess for the first time the performance of satellite based products of aerosol asymmetry parameter over broad regions of special climatic interest. Our results can offer an interesting way to assess the uncertainty induced by the use of such satellite g_{aer} data in climate and radiative transfer models that compute aerosol radiative and climate effects. The obtained results are relatively satisfactory given the difficulties encountered by satellite retrieval algorithms due to the different assumptions they made. The identified weaknesses may provide an opportunity to improve such satellite retrievals of aerosol asymmetry parameter in forthcoming data products like those of MODIS C006.

Acknowledgements. This research has been co-financed by the European Union (European Social Fund – ESF) and Greek national funds through the operational programme "Education and Lifelong Learning" of the National Strategic Reference Framework (NSRF) – Research Funding Program: THALES. Investing in knowledge society through the European Social Fund. The Collection 005 MODIS-Terra data were obtained from NASA's Level 1 and Atmosphere

Archive and Distribution System (LAADS) website (ftp://ladsweb.nascom.nasa.gov/). We would like to thank the principal investigators maintaining the AERONET sites used in the present work.

References

Barnaba, F. and Gobbi, G. P.: Aerosol seasonal variability over the Mediterranean region and relative impact of maritime, continental and Saharan dust particles over the basin from MODIS data in the year 2001, Atmos. Chem. Phys., 4, 2367–2391, doi:10.5194/acp-4-2367-2004, 2004.

Bi, J., Huang, J., Fu, Q., Wanga, X., Shi, J., Zhang, W., Huang, Z., and Zhang, B.: Toward characterization of the aerosol optical properties over Loess Plateau of Northwestern China, Jo. Quant. Spectrosc. Ra. Trans., 112, 346–360, 2011.

Chubarova, N. Y.: Seasonal distribution of aerosol properties over Europe and their impact on UV irradiance, Atmos. Meas. Tech., 2, 593–608, doi:10.5194/amt-2-593-2009, 2009.

Di Iorio, T., di Sarra, A., Junkermann, W., Cacciani, M., Fiocco, G., and Fua, D.: Tropospheric aerosols in the Mediterranean: 1. Microphysical and optical properties, J. Geophys. Res., 108, 4316, doi:10.1029/2002JD002815, 2003.

Dubovik, O. and King, M. D.: A flexible inversion algorithm for retrieval of aerosol optical properties from Sun and sky radiance measurements, J. Geophys. Res., 105, 20673–20696, 2000.

Dubovik, O., Holben, B., Eck, T. F., Smirnov, A., Kaufman, Y. J., King, M. D., Tanré, D., and Slutsker, I.: Variability of Absorption and Optical Properties of Key Aerosol Types Observed in Worldwide Locations, J. Atmos. Sci., 59, 590–608, 2002.

Fotiadi, A., Hatzianastassiou, N., Drakakis, E., Matsoukas, C., Pavlakis, K. G., Hatzidimitriou, D., Gerasopoulos, E., Mihalopoulos, N., and Vardavas, I.: Aerosol physical and optical properties in the Eastern Mediterranean Basin, Crete, from Aerosol Robotic Network data, Atmos. Chem. Phys., 6, 5399–5413, doi:10.5194/acp-6-5399-2006, 2006.

Gerasopoulos, E., Kouvarakis, G., Babasakalis, P., Vrekoussis, M., Putaud, J. P., and Mihalopoulos, N.: Origin and variability of particulate matter (PM10) mass concentrations over the Eastern Mediterranean, Atmos. Environ., 40, 4679–4690, 2006.

ACPD
14, 22677–22713, 2014

Gkikas, A., Hatzianastassiou, N., and Mihalopoulos, N.: Study and characterization of aerosol episodes in the Mediterranean basin for the 7-year period 2000–2007 based on MODIS data, European Aerosol Conference, Greece, Thessaloniki, 24–29 August 2008.

Gkikas, A., Hatzianastassiou, N., and Mihalopoulos, N.: Aerosol events in the broader Mediterranean basin based on 7-year (2000–2007) MODIS C005 data, Ann. Geophys., 27, 3509–3522, doi:10.5194/angeo-27-3509-2009, 2009.

Gkikas, A., Hatzianastassiou, N., Mihalopoulos, N., Katsoulis, V., Kazadzis, S., Pey, J., Querol, X., and Torres, O.: The regime of intense desert dust episodes in the Mediterranean based on contemporary satellite observations and ground measurements, Atmos. Chem. Phys., 13, 12135–12154, doi:10.5194/acp-13-12135-2013, 2013.

Goloub, P. and Arino, O.: Verification of the consistency of POLDER aerosol index over land with ATSR-2 fire product, Geophys. Res. Lett., 27, 899–902, 2000.

Graßl, H.: Possible changes of planetary albedo due to aerosol particles, in: Man's Impact on Climate, edited by: Bach, W., Pankrath, J., and Kellogg, W., Elsevier, New York, 229–242, 1979.

Hansen, J., Sato, M., and Ruedy, R.: Radiative forcing and climate response, J. Geophys. Res., 102, 6831–6864, 1997.

Hatzianastassiou, N., Katsoulis, B., and Vardavas, I.: Sensitivity analysis of aerosol direct radiative forcing in ultraviolet – visible wavelengths and consequences for the heat budget, Tellus, 56b, 368–381, 2004.

Hatzianastassiou, N., Gkikas, A., Mihalopoulos, N., Torres, O., and Katsoulis, B. D.: Natural versus anthropogenic aerosols in the eastern Mediterranean basin derived from multiyear TOMS and MODIS satellite data, J. Geophys. Res., 114, D24202, doi:10.1029/2009JD011982, 2009.

Haywood, J. M. and Boucher, O.: Estimates of the direct and indirect radiative forcing due to tropospheric aerosols: A review, Rev. Geophys., 38, 513–543, 2000.

Heishman, J.: Commanding Officer, Forecaster's Handbook, U.S. Navy Cent. Meteorol., and Oceanogr. Cent., Manama, Bahrain, 1999.

Holben, B. N., Eck, T. F.,Slutsker, I., Tanré, D., Buis, J. P. , Setzer, A., Vermote, E., Reagan, J. A., Kaufman, Y., Nakajima, T., Lavenu, F., Jankowiak, I., and Smirnov, A.: AERONET – A federated instrument network and data archive for aerosol characterization, Remote Sens. Environ., 66, 1–16, 1998.

ACPD
14, 22677–22713, 2014

Evaluation of MODIS aerosol asymmetry against AERONET measurements

M. B. Korras-Carraca et al.

Ichoku, C., Chu, A. D., Mattoo, S., Kaufman, Y. J., Remer, L. A., Tanré, D., Slutsker, I., and Brent, H.: A spatio-temporal approach for global validation and analysis of MODIS aerosol products, Geophys. Res. Lett., 29, MOD1-1–MOD1-4, doi:10.1029/2001GL013206, 2002.
IPCC: Climate Change 2007: The Physical Science Basis. Contribution of Working Group I to the Fourth Assessment Report of the Intergovernmental Panel on Climate Change, edited by: Solomon, S., Qin, D., Manning, M., Chen, Z., Marquis, M., Averyt, K. B.,Tignor, M., and Miller, H. L., Cambridge University Press, Cambridge, UK and New York, NY, USA, 2007.
IPCC: Climate Change 2013: The Physical Science Basis. Contribution of Working Group I to the Fifth Assessment Report of the Intergovernmental Panel on Climate Change, edited by: Stocker, T. F., Qin, D., Plattner, G.-K., Tignor, M., Allen, S. K., Boschung, J., Nauels, A., Xia, Y., Bex, V., and Midgley, P. M., Cambridge University Press, Cambridge, United Kingdom and New York, NY, USA, 1535 pp., 2013.
Kalivitis, N., Gerasopoulos, E., Vrekoussis, M., Kouvarakis, G., Kubilay, N., Hatzianastassiou, N., Vardavas, I., and Mihalopoulos, N.: Dust transport over the eastern Mediterranean derived from TOMS, AERONET and surface measurements, J. Geophys. Res., 112, D03202, doi:10.1029/2006JD007510, 2007.
Kaufman, Y. J., Tanré, D., Remer, L. A., Vermote, E. F., Chu, A., and Holben, B. N.: Operational remote sensing of tropospheric aerosol over land from EOS moderate resolution imaging spectroradiometer, J. Geophys. Res., 102, 17051– 17067, 1997.
Kinne, S., O'Donnel, D., Stier, P., Kloster, S., Zhang, K., Schmidt, H., Rast, S., Giorgetta, M., Eck, T. F., and Stevens, B.: MAC-v1: A new global aerosol climatology for climate studies, J. Adv. Model. Earth Syst., 5, 704–740, doi:10.1002/jame.20035, 2013.
Koepke, P., Hess, M., Schult, I., and Shettle, E. P.: Global aerosol data set, Rep. No. 243, Max-Planck Institut fuer Meteorologie, Hamburg, Germany, 44 pp., 1997.
Lelieveld, J., Berresheim, H., Borrmann, S., et al.: Global air pollution crossroads over the Mediterranean, Science, 298, 794–799, doi:10.1126/science.1075457, 2002.
Lohmann, U. and Feichter, J.: Global indirect aerosol effects: a review, Atmos. Chem. Phys., 5, 715–737, doi:10.5194/acp-5-715-2005, 2005.
Lyamani, H., Olmo, F. J., Alcántara, A., and Alados-Arboledas, L.: Atmospheric aerosols during the 2003 heat wave in southeastern Spain. I: Spectral optical depth, Atmos. Environ., 40, 6453–6464, doi:10.1016/j.atmosenv.2006.04.048, 2006.

ACPD
14, 22677–22713, 2014

Pace, G., di Sarra, A., Meloni, D., Piacentino, S., and Chamard, P.: Aerosol optical properties at Lampedusa (Central Mediterranean). 1. Influence of transport and identification of different aerosol types, Atmos. Chem. Phys., 6, 697–713, doi:10.5194/acp-6-697-2006, 2006.
Pandithurai, G., Pinker, R. T., Devara, P. C. S., Takamura, T., and Dani, K. K.: Seasonal asymmetry in diurnal variation of aerosol optical characteristics over Pune, western India, J. Geophys. Res., 112, D08208, doi:10.1029/2006JD007803, 2007.
Papadimas, C. D., Hatzianastassiou, N., Mihalopoulos, N., Querol, X., and Vardavas, I.: Spatial and temporal variability in aerosol properties over the Mediterranean basin based on 6-year (2000–2006) MODIS data, J. Geophys. Res., 113, D11205, doi:10.1029/2007JD009189, 2008.
Prospero, J., Ginoux, P., Torres, O., and Nicholson, S. E.: Environmental Characterization of Global sources of atmospheric soil dust derived from the NIMBUS-7 TOMS absorbing aerosol product, Rev. Geophys., 40, 1002, doi:10.1029/2000RG000095, 2002.
Remer, L. A., Kaufman, Y. J., Tanré, D., Mattoo, S., Chu, D. A., Martins, J. V., Li, R.-R., Ichoku, C., Levy, R. C., Kleidman, R. G., Eck, T. F., Vermote, E., and Holben, B. N.: The MODIS aerosol algorithm, products, and validation, J. Atmos. Sci., 62, 947–973, 2005.
Remer, L. A., Kleidman, R. G., Levy, R. C., Kaufman, Y. J., Tanré, D., Mattoo, S., Martins, J. V., Ichoku, C., Koren, I., Yu, H., and Holben, B. N.: Global aerosol climatology from the MODIS satellite sensors, J. Geophys. Res., 113, D14S07, doi:10.1029/2007JD009661, 2008.
Satheesh, S. K., Ramanathan, V., Li-Jones, X., Lobert, J. M., Podgorny, I. A., Prospero, J. M., Holben, B. N., and Loeb, N. G.: A model for the natural and anthropogenic aerosols over the tropical Indian Ocean derived from Indian Ocean Experiment data, J. Geophys. Res., 104, 27421–27440, 1999.
Savoie, D. L., Prospero, J. M., and Nees, R. T.: Nitrate, nonsea-salt sulfate, and mineral aerosolover the northwestern Indian Ocean, J. Geophys. Res., 92, 933–942, 1987.
Sciare, J., Bardouki, H., Moulin, C., and Mihalopoulos, N.: Aerosol sources and their contribution to the chemical composition of aerosols in the Eastern Mediterranean Sea during summertime, Atmos. Chem. Phys., 3, 291–302, doi:10.5194/acp-3-291-2003, 2003.
Smirnov, A., Holben, B. N., Kaufman, Y. J., Dubovik, O., Eck, T. F., Slutsker, I., Pietras, C., and Halthore, R. N.: Optical properties of atmospheric aerosol in maritime environments, J. Atmos. Sci., 59, 501–523, 2002b.

Smirnov, A., Holben, B. N., Eck, T. F., Slutsker, I., Chatenet, B., and Pinker, R. T.: Diurnal variability of aerosol optical depth observed at AERONET (Aerosol Robotic Network) sites, Geophys. Res. Lett., 29, 2115, doi:10.1029/2002GL016305, 2002c.

Smirnov, A., Holben, B. N., Dubovik, O., O'Neill, N. T., Eck, T. F., Westphal, D. L., Goroch, A. K., Pietras, C., and Slutsker, I.: Atmospheric aerosol optical properties in the Persian Gulf, J. Atmos. Sci., 59, 620–634, 2002a.

Tanré, D., Kaufman, Y. J., Herman, M., and Mattoo, S.: Remote sensing of aerosol properties over oceans using the MODIS/EOS spectral radiances, J. Geophys. Res., 102, 16971–16988, 1997.

Tindale, N. W. and Pease, P. P.: Aerosols over the Arabian Sea: Atmospheric transport pathways and concentrations of dust and sea salt, Deep Sea Res., 46, 1577–1595, 1999.

Yu, H., Dickinson, R. E., Chin, M., Kaufman, Y. J., Holben, B. N., Geogdzhayev, I. V., and Mishchenko, M. I.: Annual cycle of global distributions of aerosol optical depth from integration of MODIS retrievals and GOCART model simulations, J. Geophys. Res., 108, 4128, doi:10.1029/2002JD002717, 2003.

Zdun, A., Rozwadowska, A., and Kratzer, S.: Seasonal variability in the optical properties of Baltic aerosols, Oceanologia, 53, 7–34, 2011.

ACPD
14, 22677–22713, 2014

Table 1. Correlation coefficients (R), mean bias, root mean squared error (RMSE) and the slope and intercept values of applied linear regression fits between MODIS and AERONET g_{aer} data. The statistical parameters are given separately for the pairs of wavelengths: (i) 470 nm (MODIS) and 440 nm (AERONET), (ii) 660 nm (MODIS) and 675 nm (AERONET) and (iii) 870 nm (MODIS and AERONET). The statistical parameters are also given separately for winter, spring, summer and autumn.

MODIS-Terra						
		R	Bias*	RMSE	Slope	Intercept
year	470–440	0.25	2×10^{-4}	0.045	0.36	0.45
	660–675	0.41	−0.028	0.060	0.55	0.32
	870	0.47	−0.035	0.070	0.60	0.29
Winter	470–440	0.20	4.5×10^{-4}	0.046	0.26	0.53
	660–675	0.35	−0.033	0.056	0.41	0.42
	870	0.41	−0.053	0.057	0.40	0.43
Spring	470–40	0.27	-5×10^{-4}	0.046	0.40	0.43
	660–675	0.44	−0.023	0.060	0.63	0.27
	870	0.50	−0.026	0.071	0.67	0.24
Summer	470–440	0.33	−0.002	0.044	0.51	0.35
	660–675	0.48	−0.031	0.061	0.71	0.22
	870	0.54	−0.030	0.077	0.79	0.16
Autumn	470–440	0.21	0.003	0.044	0.30	0.50
	660–675	0.33	−0.027	0.059	0.45	0.38
	870	0.41	−0.035	0.068	0.53	0.34

ACPD
14, 22677–22713, 2014

Evaluation of MODIS aerosol asymmetry against AERONET measurements

M. B. Korras-Carraca et al.

Table 1. Continued.

MODIS-Aqua						
		R	Bias*	RMSE	Slope	Intercept
	470–440	0.27	0.018	0.047	0.41	0.40
	660–675	0.42	−0.005	0.062	0.61	0.26
	870	0.46	−0.015	0.072	0.61	0.26
Winter	470–440	0.25	0.024	0.049	0.36	0.43
	660–675	0.39	−0.001	0.062	0.55	0.30
	870	0.43	−0.021	0.068	0.51	0.33
Spring	470–440	0.29	0.015	0.048	0.45	0.38
	660–675	0.45	−0.003	0.064	0.70	0.20
	870	0.50	−0.007	0.076	0.71	0.19
Summer	470–440	0.35	0.014	0.045	0.55	0.30
	660–675	0.50	−0.012	0.060	0.72	0.19
	870	0.53	−0.018	0.074	0.73	0.19
Autumn	470–440	0.20	0.021	0.047	0.30	0.47
	660–675	0.32	−0.003	0.061	0.46	0.36
	870	0.37	−0.014	0.069	0.48	0.34

* gaer(AERONET)-gaer(MODIS)

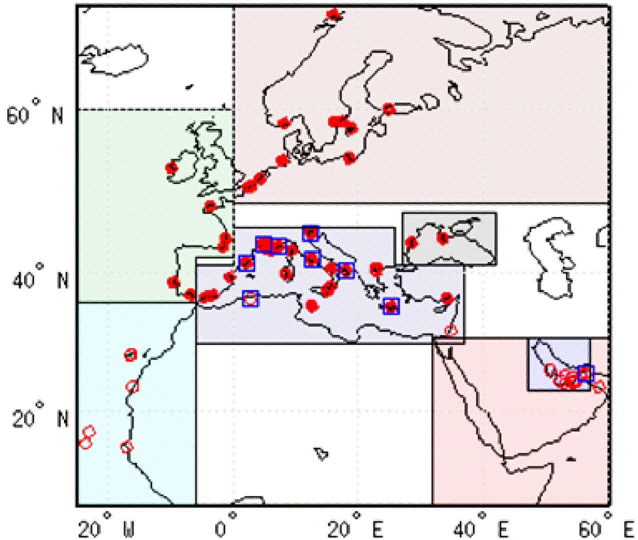

Figure 1. The study region (5° N–70° N, 25° W–60° E) and the location of 69 AERONET stations used for validation of MODIS satellite aerosol asymmetry parameter (g_{aer}) data. Solid red circles denote stations located in Europe and hollow red circles are stations in Africa, Middle East and the Arabian peninsula. The nine stations inscribed in blue squares have high AERONET and MODIS g_{aer} data availability and therefore selected for examining g_{aer} temporal tendencies. Also shown are seven sub-regions selected for studying the seasonal variation of g_{aer}.

ACPD
14, 22677–22713, 2014

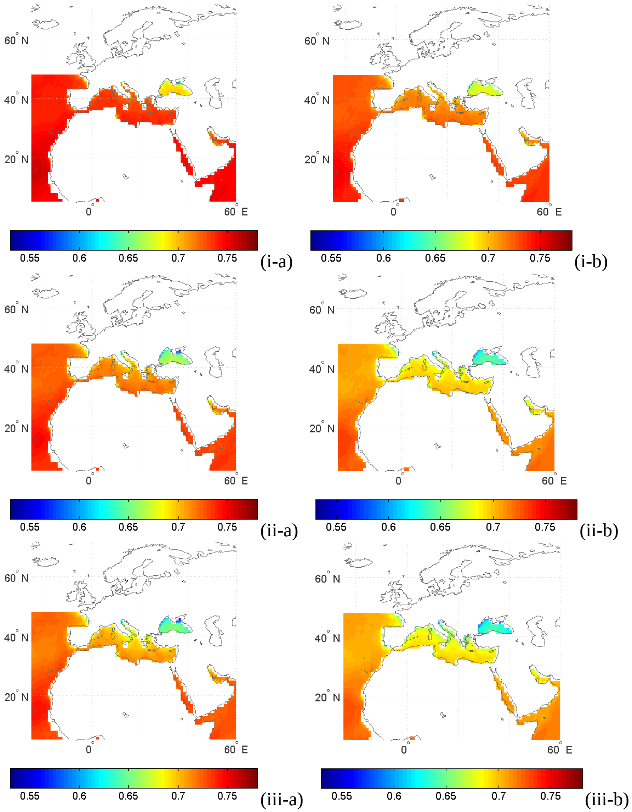

Figure 2. Geographical distribution of MODIS-Terra (**-a**, left column) and MODIS-Aqua (**-b**, right column) g_{aer} values averaged over 2002–2010, at the wavelengths of: 470 nm (**i-**, top row), 660 nm (**ii-**, middle row) and 870 nm (**iii-**, bottom row).

ACPD
14, 22677–22713, 2014

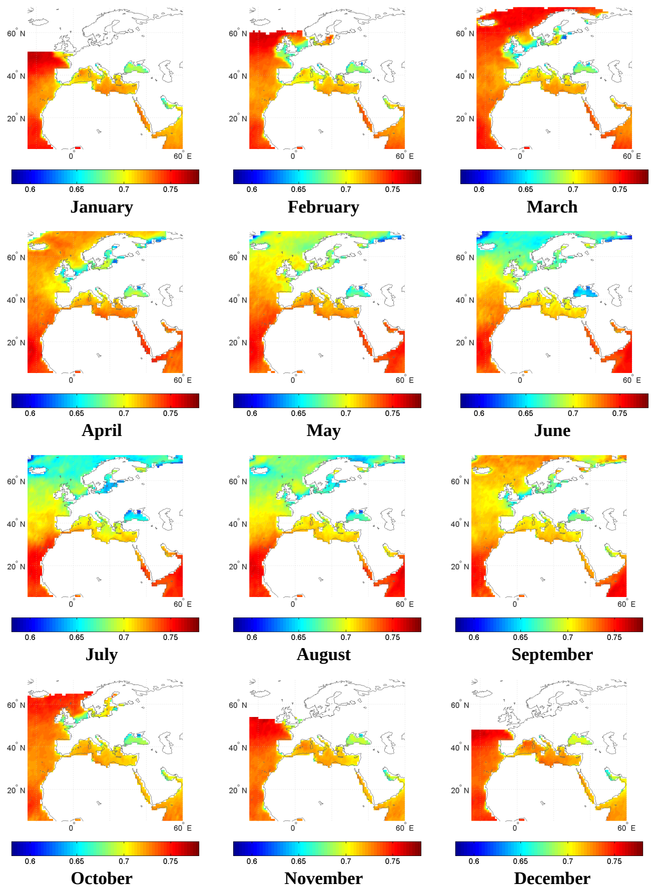

Figure 3. Month by month variation of MODIS-Aqua g_{aer} values at 470 nm averaged over the period 2002–2010.

ACPD
14, 22677–22713, 2014

Evaluation of MODIS aerosol asymmetry against AERONET measurements

M. B. Korras-Carraca et al.

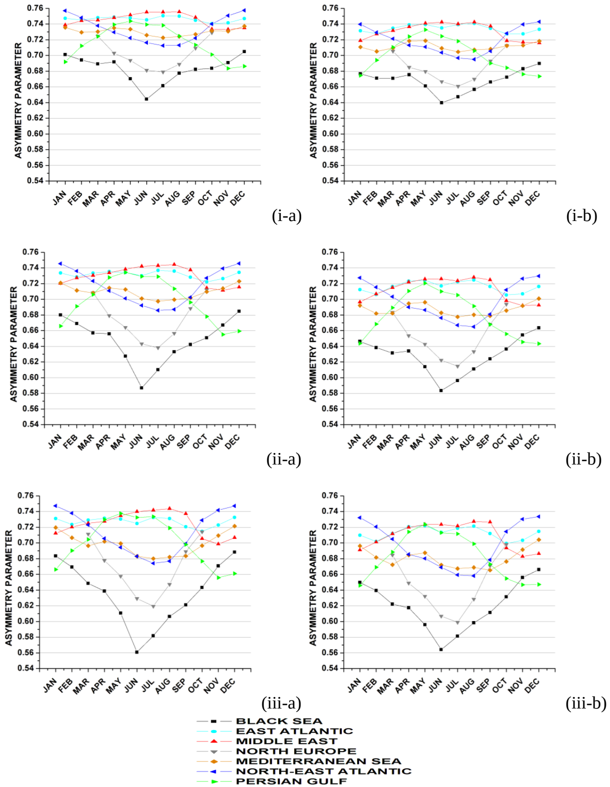

Figure 4. Intra-annual variation of MODIS Terra (**-a**, left column) and Aqua (**-b**, right column) g_{aer} values averaged over seven selected sub-regions (Fig. 1). Results are given for g_{aer} values at: 470 nm (**i-**, top row), 660 nm (**ii-**, middle row) and 870 nm (**iii-**, bottom row), averaged over the period 2002–2010.

ACPD
14, 22677–22713, 2014

Evaluation of MODIS aerosol asymmetry against AERONET measurements

M. B. Korras-Carraca et al.

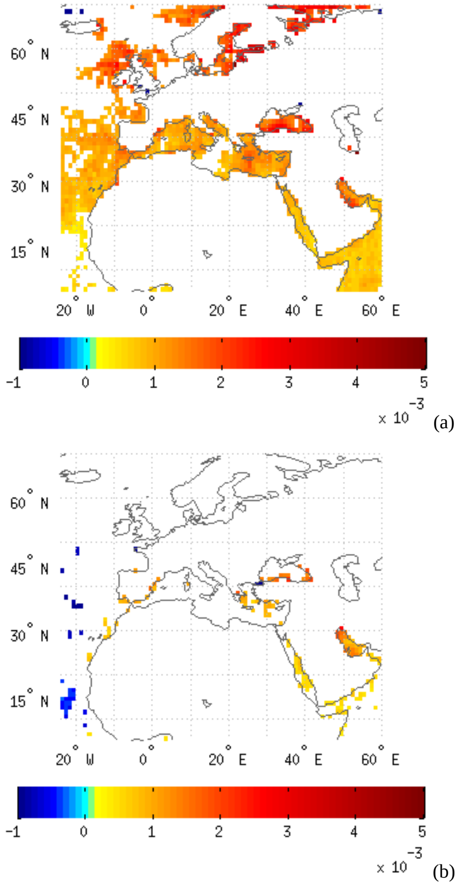

Figure 5. Slope(in units decade^{-1}) of MODIS g_{aer} deseasonalized anomalies over the period 2002–2010 from MODIS-Terra (**-a**, top) and MODIS-Aqua (**-b**, bottom), for the wavelength of 470 nm.

ACPD
14, 22677–22713, 2014

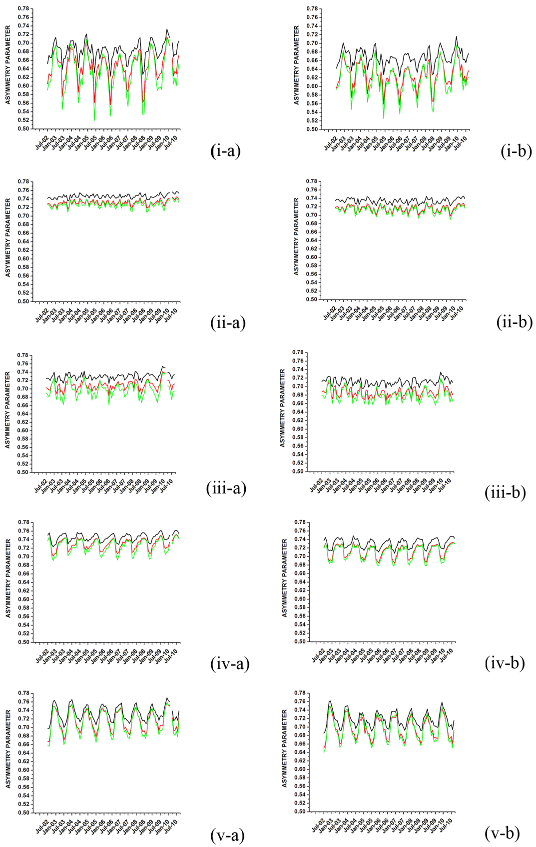

Figure 6. Inter-annual (2002–2010) variation of monthly mean g_{aer} values at 470 nm (black lines), 660 nm (red lines) and 870 nm (green lines), averaged over the sub-regions of: **(i)** Black Sea, **(ii)** Eastern Atlantic Ocean, **(iii)** Mediterranean Sea, **(iv)** Middle East, **(v)** North-eastern Atlantic Ocean, **(vi)** North Europe and **(vii)** Persian Gulf. Results are given based on MODIS-Terra (**-a**, left column) and MODIS-Aqua (**-b**, right column).

ACPD
14, 22677–22713, 2014

Evaluation of MODIS aerosol asymmetry against AERONET measurements

M. B. Korras-Carraca et al.

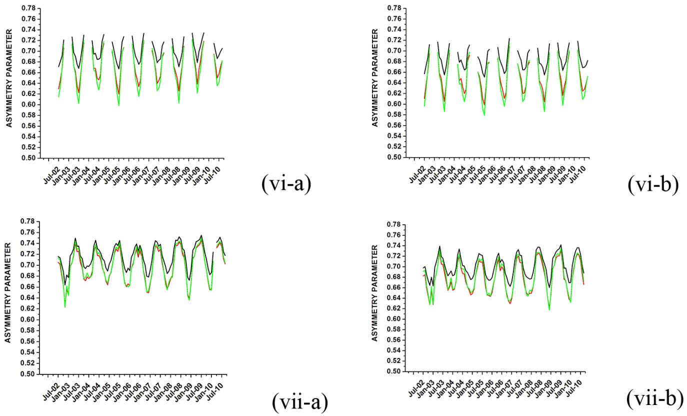

Figure 6. Continued.

ACPD
14, 22677–22713, 2014

Evaluation of MODIS aerosol asymmetry against AERONET measurements

M. B. Korras-Carraca et al.

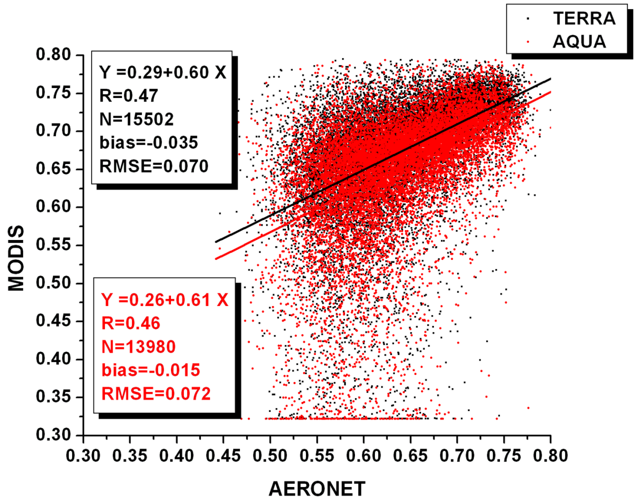

Figure 7. Scatterplot comparison between g_{aer} values at 870 nm from MODIS Terra (black color) and Aqua (red color) and corresponding values from AERONET stations (blue squares, Fig. 1). The correlation coefficients (R), mean bias, root mean squared error and the slope and intercept of applied linear regression fits between MODIS and AERONET data are given.

ACPD
14, 22677–22713, 2014

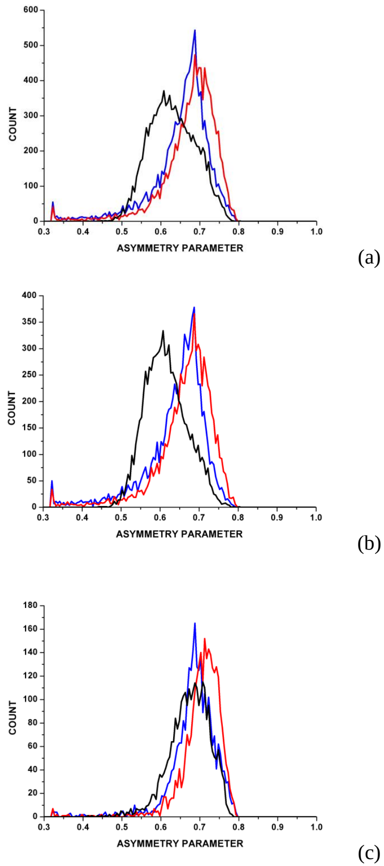

Figure 8. Frequency distribution histograms for MODIS-Terra (red colored lines) MODIS-Aqua (blue-colored lines) and AERONET (black lines) g_{aer} values at 870 nm. The histograms are given separately for: **(a)** the entire study region, **(b)** Europe and **(c)** Africa, Middle East and Arabian peninsula.

ACPD
14, 22677–22713, 2014

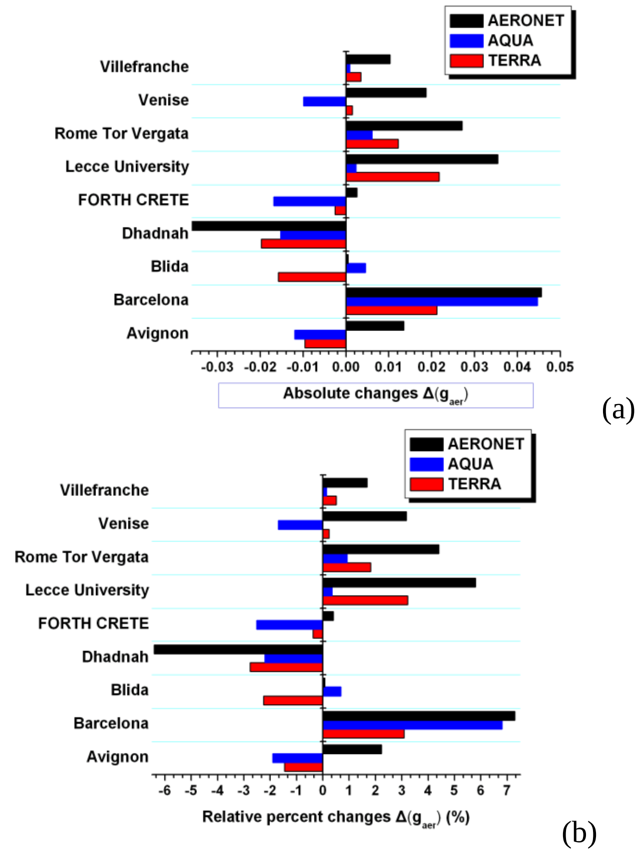

Figure 9. Absolute **(a)** and relative percent **(b)** changes of g_{aer} values at 870 nm based on MODIS-Terra (red color), MODIS-Aqua (blue color) and AERONET (black color) data. The comparison is given for nine selected stations (contained in blue squares in Fig. 1).

ACPD
14, 22677–22713, 2014

Evaluation of MODIS aerosol asymmetry against AERONET measurements

M. B. Korras-Carraca et al.

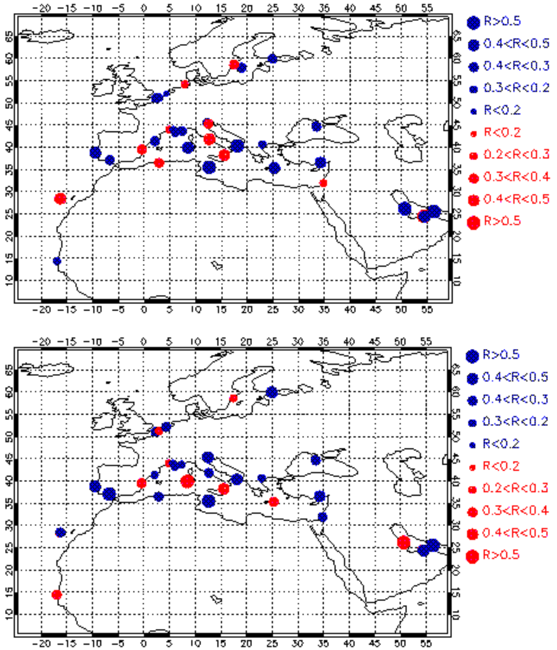

(a)

(b)

Figure 10. Map distribution of correlation coefficients between: MODIS-Terra and AERONET g_{aer} values at 870 nm **(a)** and MODIS-Aqua and AERONET g_{aer} values at 870 nm **(b)**. The size of circles corresponds to the magnitude of correlation coefficients, while blue and red colors are used for stations for which MODIS and AERONET indicate same and opposite tendency g_{aer}, respectively.

ACPD
14, 22677–22713, 2014